Mass Transfer in an Adiabatic Rectifier of Ammonia-Water Absorption System

Byong Joo kim*

Key words : Adiabatic rectification process, Falling film, Heat and mass transfer, Rectification efficiency

Abstract

Falling film rectification involves simultaneous heat and mass transfer between vapor and solution film. In the present work, the adiabatic rectification process of ammonia-water vapor by the falling solution film on the vertical plate was investigated. The continuity, momentum, energy and diffusion equations for the solution film and the vapor mixture were formulated in integral forms and solved numerically. The model could predict the film thickness, the pressure gradient, and the mass transfer rate. The effects of Reynolds number and ammonia concentration of solution and vapor mixture, rectifier length, and the enhancement of mass transfer coefficient in each phases were investigated. The stripping of water in vapor mixture occurred near the entrance of ammonia solution, which imposed the proper size of an adiabatic rectifier. Rectifier efficiency increased as film Reynolds number increased and as vapor mixture Reynolds number decreased. The improvement of rectifer efficiency was significant with the enhancement of mass transfer coefficient in falling film.

Nomenclature

A : Heat transfer area [m²]
C : Mass concentration of ammonia
D : Mass diffusivity [m²/s]
e : Internal energy [kJ/kg]
f : Friction factor
g : Gravitational acceleration [m/S^2]
H : Gap between plates [m]
h : Convective heat transfer coef. [W/m²K]
i : Enthalpy [kJ/kg]
k : Thermal conductivity [W/mK]
K : Diffusion mass transfer coefficient [m/s]
L : Heat of absorption [kJ/kg]

* Department of Mechanical Engineering, Hongik University, Seoul 121-791, Korea

$\dot{m}''$: Mass flux [kg/m²s]
p : Pressure [Pa]
q : Heat transfer rate [W]
Re : Reynolds number
T : Temperature [℃]
t : Time [s]
u : Velocity in streamwise direction [m/s]
x : Axial coordinate [m]
y : Coordinate perpendicular to flow direction [m]
z : Mass fraction of ammonia in rectification flux

Greek symbols

α : Void fraction
δ : Solution film thickness [m]
Δ : Concentration boundary layer thickness in solution film [m]
η : Efficiency
μ : Viscosity [Ns/m²]
ρ : Density [kg/m³]
τ : Shear force [N]

Superscript

′ : per unit length
″ : per unit area

Subscript

b : Bulk mean
e : Exit
eq : Thermodynamic equilibrium
f : Solution film
g : Vapor mixture
i : Inlet
o : Base-line condition
s : Liquid-vapor interface
w : Wall

I. Introduction

Absorption cooling/heating technology is currently experiencing a resurgence of interest since the observation of ozone depletion by CFCs in stratosphere. The abrupt increase of electric peak load for air conditioning during summer also strongly encourages the use of heat-operated cooling system such as water-LiBr or ammonia-water absorption system.

In ammonia-water absorption cooling/heating system, the vapor generated in the generator contains a certain amount of water. The mass fraction of vapor mixture depends on the mass fraction of the liquid mixture the temperature and the design of generator. Any water contained in vapor is detrimental to the performace of the system. It is necessary to remove water vapor from ammonia-water vapor mixture that is regenerated in the generator. One way to remove water vapor from an ammonia-water vapor mixture is to use a counter-flow purification column. The solution is flowing from the top to the bottom, while the vapor generated, in contact with solution, flows in counter-flow from the bottom to the top, which is called the rectification process. As a result of heat and mass exchange between phases in counter-current flow, the concentration of the ammonia-water vapor mixture could be substantially increased at the exit. Thus careful rectifier design that limits the carryover of water and brings the leaving vapor contact with the entering rich solution is quite important for the improvement of system efficiency.

Various experimental and theoretical investigations on the heat and mass transfer characteristics between the falling film and vapor were conducted in conjunction with condensation and absorption process. Stephan[1] an-

alysed the condensation and rectification process of multicomponent vapor mixture. Bannwart and Bontemps[2] developed the gas phase model to study the effect of film thickness on the mass transfer. Arman and Panchal[3] proposed semi-empirical model on the absorption process of ammonia-water vapor into the falling film. Kim[4] analysed the absorption process of the falling film numerically. However systematic and quantitative research on the rectification process is very hard to find. Recently Tsujimori et al.[5,6] studied the effects of vapor flow rate and ammonia mass concentration of solution on rectifying performance experimentally and compared to their simple model.

In the present study the mass transfer in plate-type adiabatic rectifier was investigated theoretically. The aim of the present study is to analyse and understand the variation of the states of solution film and the vapor mixture along the rectification process. The velocity, temperature and the concentration profile in the ammonia solution film and the ammonia-water vapor mixture were solved by using integral method, which resulted in the mass transfer rate for given conditions and the rectification efficiency

2. Model and Governing Equations

The analysis of mass transfer during the rectification process of a binary mixture of ammonia and water includes the predictions of the local momentum, heat, and mass transfer rates and the integration of the conservation equations. Meanwhile, the constitutive relations, such as the continuity of transport variables as well as their flux at the liquid-vapor interface should be satisfied.

Figure 1 depicts the schematic of a falling film on a vertical plate and the coordinate system. Falling film of liquid solution flows down over a solid surface of given geometry by gravity. The vapor flows counter-currently with the falling film. The vapor mixture of ammonia and water condenses at the liquid-vapor interface and each component diffuses into the film depending upon its concentration gradient.

The following assumptions have been made in formulating the model.

(1) The thermo-physical properties of liquid solution and vapor mixture are constant.
(2) Thermodynamic equilibrium prevails at the liquid-vapor interface.
(3) Both phases are binary mixture of ammonia and water in the absence of non-absorbable gases.
(4) The solution film is laminar with smooth vapor-liquid interface, where interfacial wave is neglected for simplification.
(5) The solution film is fully-developed hydrodynamically and thermally but the concentration boundary layer is developing.

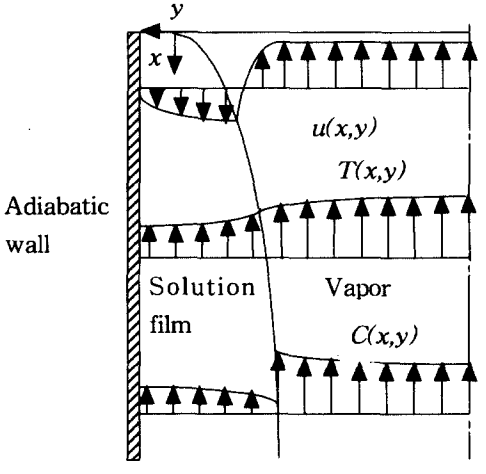

Fig. 1 Schematic picture of a falling film in an adiabatic plate rectifier.

(6) The vapor mixture is either laminar or turbulent flow with uniform-plug profile for its velocity, temperature, and concentration.
(7) There is no slip between phases.
(8) Thermal diffusion, diffusion-induced thermal effects and interdiffusion are negligible.

The hydrodynamic and thermal boundary layers develop immediately after the solution is introduced into the rectifier due to its thin film thickness. However, unlike the vapor mixture, the solution concentration boundary layer should be developing since the Schmidt number (~100) is much bigger than the Prandtl number (~1).

Under these assumptions, the mass transfer process in the rectifier is governed by the mass, momentum, energy and diffusion (mass conservation for ammonia species) equations of the solution and vapor. The integral forms of these equations for the solution film are

$$\frac{\partial}{\partial t}\int \rho_f dA_f + \frac{\partial}{\partial z}\int \rho_f u_f dA_f = \dot{m}' \tag{1}$$

$$\frac{\partial}{\partial t}\int \rho_f u_f dA_f - u_s\frac{\partial}{\partial t}\int \rho_f dA_f + \frac{\partial}{\partial z}\int \rho_f u_f^2 dA_f - u_s\frac{\partial}{\partial z}\int \rho_f u_f dA_f = -\left(\frac{\partial p}{\partial z} - \rho_f\right)\int dA_f + \tau_w' - \tau_s' \tag{2}$$

$$\frac{\partial}{\partial t}\int \rho_f e_f dA_f - e_{fs}\frac{\partial}{\partial t}\int \rho_f dA_f + \frac{\partial}{\partial z}\int \rho_f u_f i_f dA_f - i_{fs}\frac{\partial}{\partial z}\int \rho_f u_f dA_f = -q_w' + q_{fs}' \tag{3}$$

$$\frac{\partial}{\partial t}\int \rho_f C_f dA_f + \frac{\partial}{\partial z}\int \rho_f u_f C_f dA_f = \dot{m}' z \tag{4}$$

where equation (4) is the continuity of ammonia in a falling film. $\dot{m}$ is the rectification rate, q the heat transfer rate, τ the shear force, e the internal energy, and i is the enthalpy. C is the mass concentration of ammonia. Superscript $'$ denotes the value per unit length of the vertical plate. Subscripts f, g, s and w denote the film, the vapor, the liquid-vapor interface and the wall respectively. z is the mass fraction of ammonia in the rectification mass flux at the liquid-vapor interface.

$$z(x) = \frac{\dot{m}'_{NH_3}}{\dot{m}'_{NH_3} + \dot{m}'_{H_2O}} \tag{5}$$

For the vapor phase the conservation equations for mass, momentum, and energy and diffusion equation become

$$\frac{\partial}{\partial t}\int \rho_g dA_g + \frac{\partial}{\partial z}\int \rho_g u_g dA_g = -\dot{m}' \tag{6}$$

$$\frac{\partial}{\partial t}\int \rho_g u_g dA_g - u_s\frac{\partial}{\partial t}\int \rho_g dA_g + \frac{\partial}{\partial z}\int \rho_g u_g^2 dA_g - u_s\frac{\partial}{\partial z}\int \rho_g u_g dA_g = -\left(\frac{\partial p}{\partial z} - \rho_g\right)\int dA_g + \tau_s' \tag{7}$$

$$\frac{\partial}{\partial t}\int \rho_g e_g dA_g - e_{gs}\frac{\partial}{\partial t}\int \rho_g dA_g + \frac{\partial}{\partial z}\int \rho_g u_g i_g dA_g - i_{gs}\frac{\partial}{\partial z}\int \rho_g u_g dA_g = -q_{gs}' \tag{8}$$

$$\frac{\partial}{\partial t}\int \rho_g C_g dA_g + \frac{\partial}{\partial z}\int \rho_g u_g C_g dA_g = -\dot{m}' z \tag{9}$$

Subscript gs denotes the liquid-vapor interface on the gas side.

Once the profiles of velocity, temperature and concentration are given, the above equations could be transformed into differential equations. Boundary conditions specified for the laminar solution film are

$$u_f(x, 0) = u_s(x) \tag{10}$$

$$u_f(x, \delta_f) = 0 \tag{11}$$

$$\mu_f \frac{\partial u_f(x,0)}{\partial y} = \tau_s'' \tag{12}$$

$$T_f(x,0) = T_s(x) \tag{13}$$

$$\frac{\partial T(x,\delta_f)}{\partial y} = 0 \tag{14}$$

$$-k_f \frac{\partial T_f(x,0)}{\partial y} = \dot{m}'' L + q_{gs}'' \tag{15}$$

$$C_f(x,0) = C_{fs}(x) \tag{16}$$

$$C_f(x,\Delta_f) = C_{fi} \tag{17}$$

$$\frac{\partial C_f(x,\Delta_f)}{\partial y} = 0 \tag{18}$$

where Δ_f is the thickness of concentration boundary layer in the solution film and L is the latent heat of vaporization. Subscript i denotes the condition at the solution inlet.

The interfacial shear stress, heat flux, and rectification mass flux, τ_s'', q_{gs}'', $\dot{m}''$, respectively, can be estimated from the characteristics of vapor flow as

$$\tau_s'' = \frac{1}{2} f_s \rho_g (u_{gb} - u_s)^2 \tag{19}$$

$$q_{gs}'' = h_g(T_{gb} - T_s) \tag{20}$$

$$\dot{m}'' = \frac{K_g(C_{gb} - C_{gs})}{z - C_{gs}} \tag{21}$$

where f is the local friction factor and subscript b denotes the bulk mean value. h_g and K_g is the interfacial heat and mass transfer coefficient for the vapor phase and can be evaluated by the Chilton-Colburn analogies[7] among mass, momentum, and energy transfer.

Velocity, temperature and concentration profiles satisfying the above boundary conditions are assumed to be parabolic, as given in equations (22), (23), and (24)

$$u_f(x,y) = u_s(1 - \frac{y^2}{\delta_f^2}) + \frac{\tau_s''}{\mu_f}(y - \frac{y^2}{\delta_f}) \tag{22}$$

$$T_f(x,y) = T_s - \frac{\dot{m}'' L + q_{gs}''}{k_f}(y - \frac{y^2}{2\delta_f}) \tag{23}$$

$$C_f(x,y) = C_{fs}(1 - \frac{2y}{\Delta_f} + \frac{y^2}{\delta_f^2}) + C_{fi}(\frac{2y}{\Delta_f} + \frac{y^2}{\delta_f^2}) \tag{24}$$

For the vapor flow, uniform-plug distributions for the velocity, temperature, and concentration profiles are adopted whether it is laminar or turbulent flow. Therefore mixed-values of velocity, temperature, and concentration of the vapor phase can be used for the formulation of equation (6)-(9).

From assumption (2), the concentration of solution and vapor at the liquid-vapor interface should satisfy the thermodynamic equilibrium condition.

$$C_{fs} = C_{f,eq}(T_s, p) \tag{25}$$

$$C_{gs} = C_{g,eq}(T_s, p) \tag{26}$$

where p is the rectifier pressure and subscript eq denotes thermodynamic equilibrium. The continuity of ammonia mass flux at the liquid-vapor interface is given by

$$C_{fs}\dot{m}'' + K_f\rho_f(C_{fs} - C_{fi}) = C_{gs}\dot{m}'' + K_g\rho_g(C_{gb} - C_{gs}) \tag{27}$$

For the solution film mass transfer coefficient could be estimated based on the concentration gradient near the interface.

$$K_f = \frac{2\rho_f D_f}{\Delta_f} \tag{28}$$

where D is the mass diffusivity of ammonia-water solution.

3. Solution Method

Due to the nonlinear nature of the conservation equations and constitutive relations, it is difficult to get solutions by solving them simultaneously. Therefore, the model is formulated with transient equations and solved until the rate of change of any variable with respect to time is negligible.

Equations (1)-(9), and equations (25), (26), (27) form a set of 12 simultaneous equations for the unknowns of δ_f, Δ_f, u_s, u_{gb}, T_s, T_{gb}, C_{fs}, C_{gs}, C_{gb}, $\dot{m}''$, z, and p. They are solved by the explicit finite difference method. Discretization of the equations using the first-order forward-time and backward-space scheme results in the difference equations. The temperature and concentration of ammonia are strongly coupled by the thermodynamic equilibrium conditions at the liquid-vapor interface. The rectification mass flux should satisfy equation (27). At the same time the temperature and ammonia concentration at the liquid-vapor interface should meet thermodynamic equilibrium conditions of equations (25) and (26). Thus, an iterative technique is used to find the interfacial temperature, concentrations, and resultant mass flux at any instant of time using the Newton method.

The results of Ziegler and Trepp[8] are used for the estimation of thermodynamic properties of ammonia-water mixture and the results of Macriss et al.[9] for the physical properties.

At each time step, calculation proceeds from the top to the bottom of the rectifier. When the rate of change of any variable with respect to time is less than the specified value, it is assumed that steady state is reached.

At the solution inlet its film thickness is assumed based on the free-falling thin film proposed by Nusselt[10]. The concentration boundary layer thickness is assumed to be very small compared to the film thickness at the solution inlet. However, provided that it is small enough, its effects on the steady-state solution shall be negligible.

4. Results and Discussion

Table 1 shows the dimensions of vertical plate rectifier and the operating conditions used in the present analysis. The ammonia solution film flows down on the vertical plate by gravity. The ammonia-water vapor mixture is assumed to be introduced to the rectifier at its bottom and flow countercurrently with the solution film. The Reynolds number of the falling film and the vapor mixture are defined as

$$Re_f = \frac{4\Gamma}{\mu_s} \tag{29}$$

Table 1 Conditions for the analysis of mass transfer in the plate-type adiabatic rectifier

Parameters	Base-line values
Plate Gap (mm)	5.0
Rectifier length (m)	0.2
System pressure (bar)	20.0
Solution inlet concentration (%)	35.0
Solution temperature (°C)	123.8
Solution Reynolds number	100
Vapor inlet concentration (%)	80.0
Vapor inlet temperature (°C)	150.8
Vapor Reynolds number	1000

$$Re_g = \frac{2\rho_g u_{gb}(H-2\delta_f)}{\mu_g} \quad (30)$$

where Γ is the solution flow rate per unit width and H is the gap between vertical plates.

Figure 2 shows the variation of the temperature of the solution, the vapor and the liquid-vapor interface. Each phase, the solution and the vapor, experiences evaporation or condensation depending upon the temperature and concentration difference between them. When the temperature of the solution film is lower than the thermodynamic equilibrium temperature of the vapor mixture, the ammonia and water species in the vapor mixture condense on the interface, whose relative mass fraction depends on the conditions. For the solution film, if the temperature of vapor mixture is higher than the thermodynamic equilibrium temperature of solution, evaporation of the more-volatile component of solution, ammonia, occurs. The higher the interfacial temeperature is, the more water species, the less-volatile component condenses and stripping process develops. Moreover sensible heat transfer from the vapor mixture to the interface since there is temperature difference. Thus the temperature of the solution film increases abruptly from the inlet in the direction of the length of the plate. However the temperature of the vapor mixture decreases as it flows upward, countercurrently with the solution film. The temperature of the liquid-vapor interface is slightly higher than the solution bulk temperature, particulary near the inlet of the plate. In the remainder of the plate the interfacial temperature is almost the same as that of the solution bulk.

Figure 3 depicts the variation of the concentration of the solution film, the vapor mixture, and the liquid-vapor interface at the liquid side and the vapor side in the direction of the plate length. Since the temperature of an interface increases sharply, the interfacial concentration at the solution side decreases due to thermodynamic equilibrium. The concentration of the vapor mixture increases as it flows from the bottom to the top of the rectifier. It is evident that the rectification proceeds since the bulk concentration of the vapor mixture increases. It can be noticed that the increase of the concentration of the vapor is significant near the inlet of the solution where the largest temperature difference exists as shown in Fig. 2.

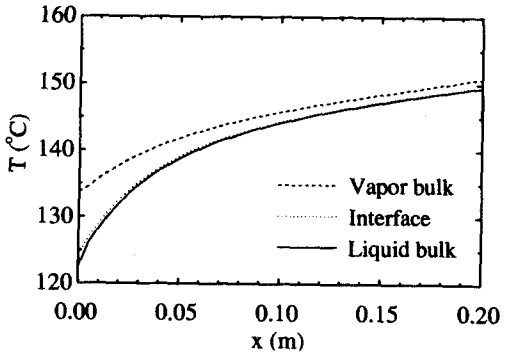

Fig. 2 Variation of local temperature along the rectifier.

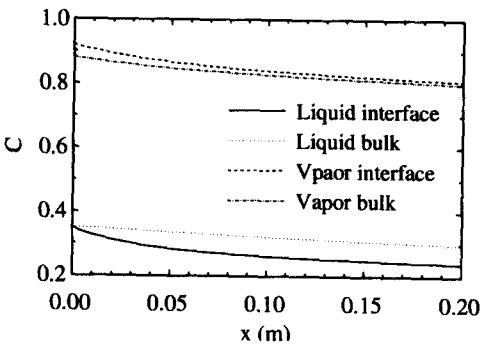

Fig. 3 Variation of local concentration of along the rectifier.

Local mass transfer rate and the mass fraction of ammonia in mass flux are given in Fig. 4 as a function of rectifier length. Mass flux consists of the ammonia and water species. Water species in the vapor mixture condenses on the interface throughout the whole rectifer. However ammonia species evaporates from the solution film to the vapor mixture in the most of the rectifier except near the solution inlet where the temperature of the solution is the lowest and the concentration difference is the biggest which results in the condensation of ammonia on the solution interface. Then the mass fraction of ammonia in the mass flux, z, is negative in the most part of the rectifier, which proves the rectification is in effect. The evaporation rate of ammonia from the solution film is almost constant in the downstream of the rectifier. It shows the decay of the evaporation rate and finally the change of mass transfer direction near the inlet of the solution. On the contrary the vapor mixture shows the exceptionally high rectification rate in the top portion of the plate. The adiabatic rectification process is dominated by the condensation of water species and the upstreams of the rectifier seems to be the most important

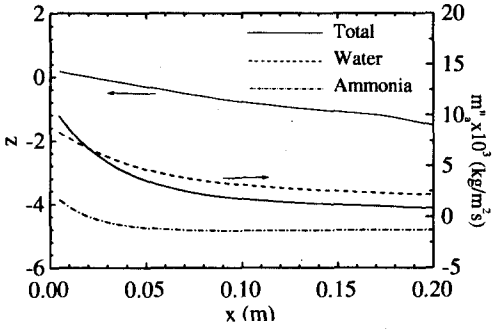

Fig. 4 Variation of local mass flux and the fraction of ammnia component.

rectification region.

The maximum concentration that the vapor mixture can reach is that in thermodynamic equilibrium with the solution at inlet. The efficiency of adiabatic rectification process can be defined as

$$\eta_{adia} = \frac{C_{gb,i} - C_{gb,e}}{C_{gs,i} - C_{gb,e}} \tag{31}$$

The change of an adiabatic rectification efficiency due to the change in the operating conditions, such as the length of the rectifier and the Reynolds number of the solution and the vapor mixture is illustrated in Fig. 5. The ratio denotes the value of the variable divided by the base-line operation conditions given in Table 1. As the length of the rectifier increases adiabatic rectification efficiency increases. However, the rate of increase in an adiabatic rectification efficiency diminishes as the rectifier length increases and converges to an almost a constant value. This is due the fact that, as explained in Fig. 4, most of the stripping occurs near the inlet of the solution.

The increase of the Reynolds number in the ammonia-water vapor mixture leads to the increase of heat and mass transfer rate from the vapor to the liquid-vapor interface due to increased transport characteristics. Sin ce the mass flow rate is increased with the Reynolds number, the rectification efficiency decreases rapidly especially at low Reynolds number. As the water species condenses on the solution film as a result of stripping, the concentration of ammonia in the solution film decreases while the concentration of water species increases and the stripping retards along the downstream of the rectifier. It can be activated by the increase of the solution Reynolds number. Figure 5 proves that the adia-

batic rectification efficiency increases with the solution film Reynolds number.

The effect of the concentration of the solution film or the vapor mixture on the rectification efficiency is shown in Fig. 6. Dimensionless concentration C^* is defined based on the base-line concentration difference.

$$C^* = \frac{C_{gb,i} - C_{fb,i}}{(C_{gb,i} - C_{fb,i})_o} \tag{32}$$

As the concentration of the solution increases at the inlet of the rectifier, dimensionless concentration difference decreases. The increase of solution concentration results in the decrease of equilibrium temperature, the decrease of the concentration difference with the vapor mixture, and the increase of the concentration of water species. Thus the rectification efficiency increases with the rapid increase of interfacial concentration. However it shows a retarding trend of efficiency since the maximum concentration that the vapor mixture reaches is determined by the thermodynamic equilibrium conditions. For the vapor mixture, if the concentration increases, dimensionless concentration difference increases and the equilibrium temperature decreases. As explained in Fig. 2 the increase of condensation rate of water species in the vapor mixture leads to the increase of the adiabatic rectification efficiency linearly.

Heat and mass transfer coefficient of the solution film and the vapor mixture, given in equations (21), (22), (27), and (28), could be enhanced by augmenting the geometrical factor or by introducing the internal mixing. The effect of the enhancement factor (EF, the ratio of transfer coefficient to its base-line value) is shown in Fig. 7. The main resistance in the transport process of falling film lies in the solution film. As the transport characteristics of the solution film increases adiabatic rectification efficiency increases abruptly. The increase of the enhancement factor in the vapor mixture also results in the increase of the rectification efficiency. However the effect of EF in the vapor mixture is smaller than that of the solution film particularly near the high EF.

5. Conclusions

In the present study the mass transfer in plate-type adiabatic rectifier was investigated theoretically. The velocity, temperature and

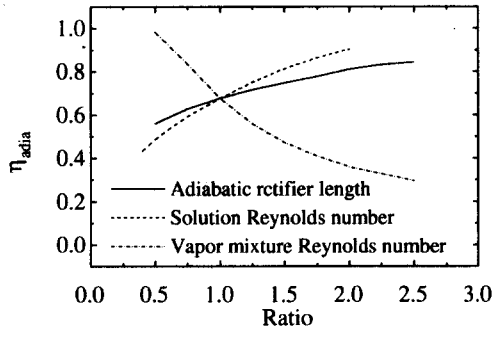

Fig. 5 Effects of rectifier length and the Reynolds number of solution and vapor mixture on an adiabatic rectifier efficiency.

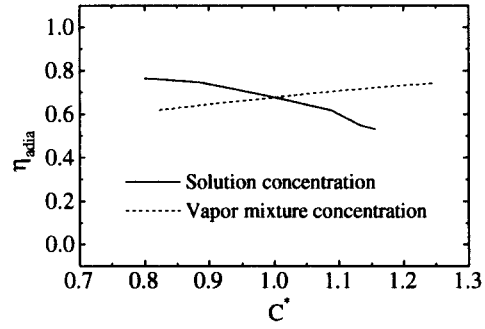

Fig. 6 Effects of solution and vapor concentration on an adiabatic rectifier efficiency.

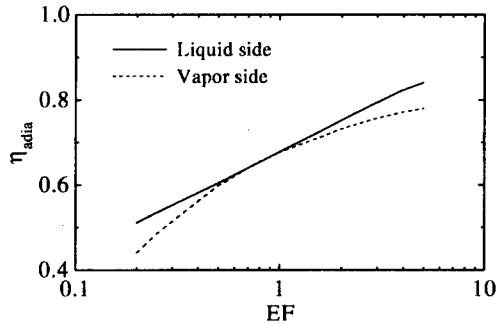

Fig. 7 Effects of enhancement in transfer coefficient of solution and vapor on adiabatic rectifier efficiency.

the concentration profile in the ammonia solution film and the ammonia-water vapor mixture were solved by using integral method. The effect of mass flow rates, concentration and the transport characteristics of the solution film and the vapor mixture on the adiabatic rectification efficiency were investigated. The conslusions are as follows:

(1) The stripping of water species in the vapor mixture occurred near the inlet of ammonia solution, which imposed the proper size of an adiabatic rectifier is important.

(2) Rectifier efficiency increased as the solution film Reynolds number increased and as the vapor mixture Reynolds number decreased.

(3) The improvement of rectifier efficiency was significant with the enhancement of mass transfer coefficient in falling film.

References

(1) Stephan, S., 1981, "Heat transfer with condensation in multicomponent mixtures, in Heat Exchangers-Thermal-hydraulic Fundamentals and Designs," Edited by Kakac, S., Bergles, A.E., and Mayinger, G., Kluwer Academic Publishers.

(2) Bannwart, A. C. and Bontemps, A., 1990, "Condensation of a vapor with incondensables : an improved gas phase film model accounting for the effect of mass transfer on film thickness," Int. J. Heat Mass Transfer, Vol. 33, No. 7, pp. 1465-1474.

(3) Arman, B. and Panchal, C. B., 1993, "Absorption analysis of ammonia in an aqueous solution," Proceedings of 28th IECEC, Vol. 1, pp. 873-878.

(4) Kim, B. J., 1998, "Heat and mass transfer in a falling film absorber of ammonia-water absorption systems," Heat Transfer Engineering-An International Quarterly, Vol. 19, No. 3, pp. 53-63.

(5) Tsujimori, A., Ozaki, E. and Nakao, K., 1997, "Performance analysis of rectifier in NH3-H2O absorption heat pump - Characteristic of packed tower-type rectifier," Trans. JSRAE, Vol. 14, No. 1, pp. 19-25.

(6) Tsujimori, A., Ozaki, E. and Nakao, K., 1997, "Performance analysis of rectifier in NH3-H2O absorption heat pump (Characteristic of enriching section of rectifier)," Trans. JSRAE, Vol. 14, No. 1, pp. 255-263.

(7) Chilton, T. H. and Colburn, A. P., 1934, "Mass transfer (absorption) coefficient, prediction from data on heat transfer and fluid friction," Ind. Eng. Chem., Vol. 26, pp. 1183-1187.

(8) Ziegler, B. and Trepp, C. H., 1984, Equation of state for ammonia-water mixtures, Int. J. Refrigeration,, Vol. 7, No. 2, pp. 101-106.

(9) Macriss, R. A., Eakin, B. E., Ellington, R. T. and Huebler, J., 1964, "Physical